Fourth International Conference on Advanced COmputational Methods in ENgineering (ACOMEN 2008)
Editors: M. Hogge, R. Van Keer, L. Noels, L. Stainier, J.-P. Ponthot, J.-F. Remacle, E. Dick

A study of complex delaminations in laminated composite structures with SAMCEF

M. Bruyneel[1], J.P. Delsemme[1*], P. Jetteur[1] and F. Germain [2]

[1]Analysis Group, SAMTECH s.a.
Liège Science Park, Angleur, Belgium

[2]SAMTECH s.a., Toulouse, France

e-mails: *{Michael.Bruyneel, Jeanpierre.Delsemme,Philippe.Jetteur}@samcef.com,*
Fabrice.Germain@toulouse.samtech.fr

Abstract

This paper describes the solution procedures available in the commercial finite element code SAMCEF for studying delaminations in composite structures, in the case of quasi static solicitations. Two approaches are presented. The first one is based on fracture mechanics and aims at computing the energy release rates by modes; the second one relies on damage and fracture mechanics and is well suited for inter-laminar crack propagation. The methods are discussed and validated on classical benchmarks (as the DCB and ENF tests) and are finally applied to a complex (industrial) case including tens of crack fronts and many contact regions.

1 Introduction

With their high stiffness to weight ratio and their anisotropic properties, composite materials are widely used in the aeronautics industry. One of the predominant modes of failure in laminated composites is delamination, resulting from a separation of adjacent layers at locations sensitive to transverse effects. A large amount of such cracks may initiate in real-life laminated structures and weaken their overall mechanical properties. It is therefore mandatory to take those flaws into account in the design phase and to check the structural integrity while they propagate.

Assessing the damage tolerance of composite structures is clearly a challenge. At least two numerical approaches have been developed to study this problem with the finite element method [1]. The first one consists in using fracture mechanics in a (possible linear) static analysis and to compute the 3 modes of the strain energy release rate along the different crack fronts in order to evaluate the critical crack [2,3,4]. Secondly, in a more advanced non linear analysis, cracks growth can be simulated by inserting cohesive elements at some interfaces between plies, where a softening material behaviour is assigned to represent the damage [5,6,7,8].

Modelling and solving such a finite element problem is difficult. An efficient numerical solution procedure should be able to easily insert multiple crack fronts in a given large scale meshed structure, and to efficiently manage not only softening material behaviours assigned to the interfaces, but also the numerous contacts that can appear between the plies. It results that most of the published works in the field present solutions for simple composite structures with a small amount of delamination sites and few contact conditions.

For solving industrial problems a finite element software code should be able to model multi-delaminated composite structures with a very large amount of cracks and to provide quickly an accurate solution. In this paper the methodology available in the SAMCEF finite element code [9,10] is applied to such a complex laminated structure including several tens of crack fronts. It is shown how easy it is to insert cracks in the mesh, and how efficiently can the numerous contact conditions be satisfied. A specific Virtual Crack Extension method is presented for computing the modes of the energy release rate, and the

---

* Part of this work was carried out under the European COCOMAT and ALCAS projects

cohesive elements method is briefly explained. Although not yet publishable experimental results have confirmed the efficiency and the accuracy of the implemented methods in an industrial case including multiple delamination sites.

2 The Virtual Crack Extension method

In SAMCEF, the VCE method is used to extract the three modes of the energy release rate G_I, G_{II} and G_{III} corresponding to the three different crack solicitations (opening, sliding and tearing modes, respectively). In VCE a direct differentiation of the total potential energy π is computed with respect to a given crack surface increment dA:

$$G_T = -\frac{d\pi}{dA} = G_I + G_{II} + G_{III} \tag{1}$$

From (2) it comes that in the elastic case the analytical derivative of the energy is calculated for nodal displacements at the equilibrium state:

$$\text{if} \qquad \pi = \frac{1}{2}\mathbf{q}^{\mathbf{T}}\mathbf{K}\mathbf{q} - \mathbf{g}^{\mathbf{T}}\mathbf{q} \qquad \text{then} \qquad \frac{d\pi}{dA} = \frac{1}{2}\mathbf{q}^{\mathbf{T}}\frac{d\mathbf{K}}{dA}\mathbf{q} - \mathbf{q}^{\mathbf{T}}\frac{d\mathbf{g}}{dA} \tag{2}$$

where **K** is the stiffness matrix, **q** and **g** are the nodal displacements and the applied forces, respectively. For the general case (possibly including geometric non linearity), (2) is rewritten as:

$$\frac{d\pi}{dA} = \frac{1}{2}\mathbf{q}^{\mathbf{T}}\frac{d\mathbf{K}}{dA}\mathbf{q} - \mathbf{q}^{\mathbf{T}}\frac{d\mathbf{g}}{dA} \quad => \quad \frac{d\pi}{dA} \cong \frac{1}{2}\mathbf{q}^{\mathbf{T}}\frac{\Delta\mathbf{K}}{\Delta A}\mathbf{q} - \mathbf{q}^{\mathbf{T}}\frac{\Delta\mathbf{g}}{\Delta A}$$
$$\frac{d\pi}{dA} \cong \frac{1}{2}\mathbf{q}^{\mathbf{T}}\frac{(\mathbf{K}_{pert} - \mathbf{K}_{init})}{\Delta A}\mathbf{q} - \mathbf{q}^{\mathbf{T}}\frac{(\mathbf{g}_{pert} - \mathbf{g}_{init})}{\Delta A}$$
$$\frac{d\pi}{dA} \cong \frac{(\pi_{pert} - \pi_{init})}{\Delta A}$$

where *pert* represents a perturbed configuration at the equilibrium. In practice (Figure 1), the nodes at the crack front are split into two. Elements on one side of the crack surface are connected to the first node, and elements on the other side to the second one. Links are written between split nodes in order to get reactions R_i (to the crack extension) at the crack front. The variation of energy in the elements touched by those nodes is computed for the displacements at the equilibrium (Figure 1c) by moving the nodes in the crack's plane. This provides $d\pi$ and the related crack advance dA. Only one finite element analysis is required to compute G_T. As the nodal displacements are considered constant (as seen in the derivative of the potential energy), and given that the mesh perturbation introduces a small crack area variation, the method is indeed a virtual crack extension. Finally, the total energy release rate is distributed on the three modes with respect to the opening energies. Sensor nodes are defined on the lips at a given distance from the crack front and measure the relative displacements U_i in the crack local axes. The total energy release rate is then weighted as follows to provide the 3 modes:

$$G_I = \frac{U_I R_I}{U_I R_I + U_{II} R_{II} + U_{III} R_{III}} G_T$$
$$G_{II} = \frac{U_{II} R_{II}}{U_I R_I + U_{II} R_{II} + U_{III} R_{III}} G_T \tag{3}$$
$$G_{III} = \frac{U_{III} R_{III}}{U_I R_I + U_{II} R_{II} + U_{III} R_{III}} G_T$$

The values of the energy release rates by mode are typically included in a criterion, e.g. (4), to decide on each crack's dangerousness and to compute the propagation load. In Eq. (4), G_{IC}, G_{IIC} and G_{IIIC} are the inter-laminar toughness, experimentally determined.

$$\frac{G_I}{G_{IC}} + \frac{G_{II}}{G_{IIC}} + \frac{G_{III}}{G_{IIIC}} = 1 \tag{4}$$

With the VCE approach it is possible to run linear static computations, providing quickly an estimation of the propagation load for a given cracked configuration. However, as this is the case for all the fracture mechanics methods, fine meshes must be defined in the vicinity of the crack fronts in order to get accurate results. This method was used for example in [11] for industrial applications.

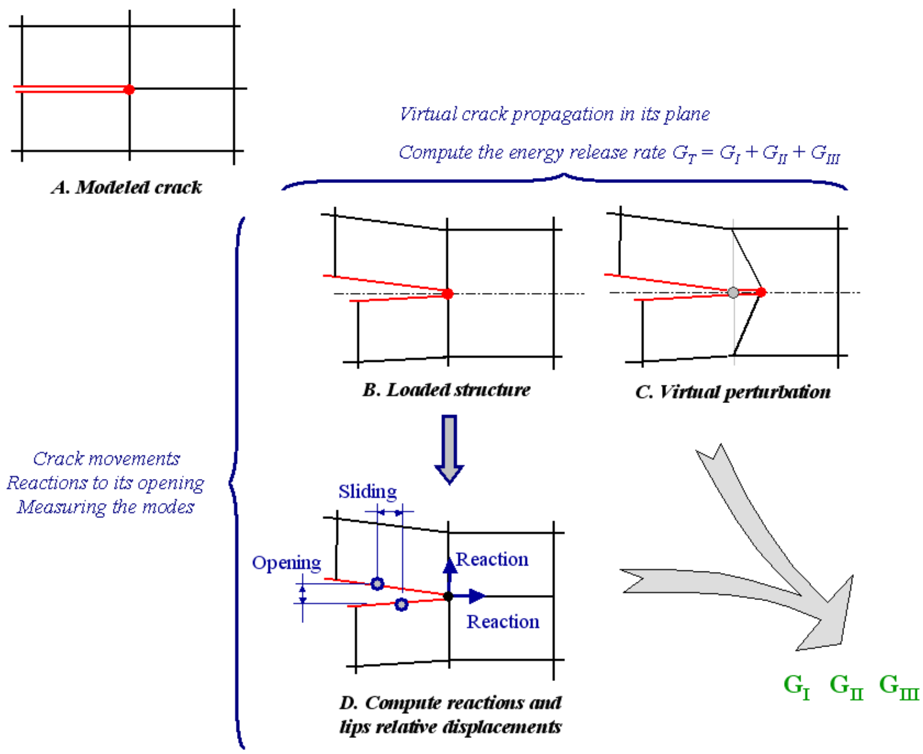

Figure 1. Principle of the VCE method in SAMCEF

3 The cohesive elements approach

In order to model the possible inter-laminar damage, a mesoscopic approach is used, where a thin layer is inserted between two plies of the laminate (Figure 2). A specific non linear softening law is assigned to the material of this thin layer, and its stiffness and strength can decrease and become equal to zero over the loading, simulating a decohesion between the plies.

The approach presented in [5] is available in SAMCEF. The related constitutive polynomial softening material law for the interface is depicted in Figure 3a. Without going into the details of [5], the constitutive equation in the interface takes the following form (5), where d is the damage variable, identical for all the directions, and k_i^0 the initial stiffness:

$$\begin{vmatrix}\sigma_{31}\\ \sigma_{32}\\ \sigma_{33}\end{vmatrix} = \begin{vmatrix} k_1^0(1-d) & & \\ & k_2^0(1-d) & \\ & & k_3^0(1-d)\end{vmatrix} \begin{vmatrix}\gamma_{31}\\ \gamma_{32}\\ \varepsilon_{33}\end{vmatrix} \tag{5}$$

When d is equal to zero the interface is intact, while $d = 1$ corresponds to an inter-laminar de-cohesion. The evolution of the damage d for the polynomial law is given by:

$$d = \left(\frac{n}{n+1} \frac{\langle Y - Y_0 \rangle_+}{Y_C - Y_0} \right)^n \qquad 0 \le d \le 1$$

where Y is an equivalent thermodynamic force, and n, Y_C are material parameters. The damage appears after a threshold Y_0 defined by the user (represented by the grey regions in Figure 3). The form of the associated fracture criterion is given in (6).

$$\left\{ \left(\frac{Y_I}{G_{IC}} \right)^\alpha + \left(\frac{Y_{II}}{G_{IIC}} \right)^\alpha + \left(\frac{Y_{III}}{G_{IIIC}} \right)^\alpha \right\}^{1/\alpha} \le \frac{Y}{Y_c} \tag{6}$$

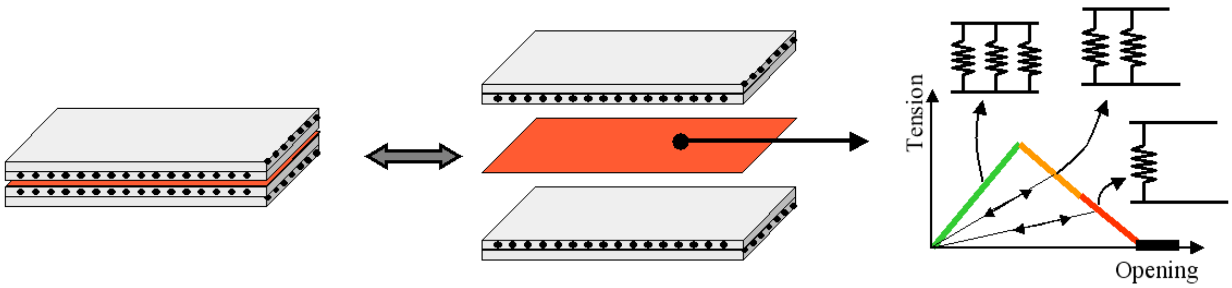

Figure 2. Inserting an interface element between two plies of a laminate

In SAMCEF a bi-triangular and an exponential laws are available as well [12]: they are illustrated in Figure 3. For the polynomial and bi-triangular cases, the damage appears after the threshold Y_0 defined by the user. For the exponential law, the damage directly appears when the interface is loaded.

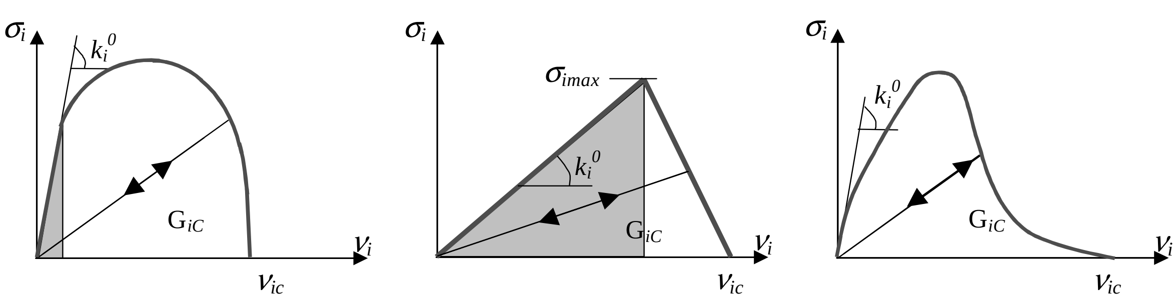

Figure 3. The constitutive softening laws available in SAMCEF for the interface elements

4 Illustration on the DCB and the ENF tests

4.1 The Double Cantilever Beam (DCB) and End Notched Flexure (ENF) tests

Those standardised tests are illustrated in Figure 4 and are often used as benchmarks in numerical applications [13]. All the computations are carried out with first order finite elements.

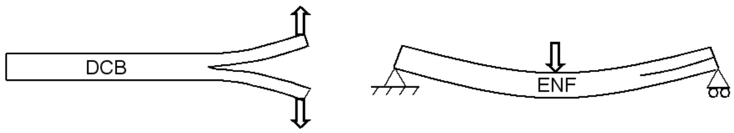

Figure 4. Illustration of the DCB and ENF tests

4.2 The DCB test solved with the VCE approach

In the configuration of Figure 5 only mode I (opening of the crack) is active. The specimen width is of 25 mm, while the crack length is 57.15 mm. A ply thickness of 0.127 mm is used, and the material is graphite/epoxy C12K/R6376. Three stacking sequences including 32 plies are tested, according to [13]:

- ❑ Unidirectional laminate: $[0]_{32}$;
- ❑ Lay-up D[++30]: $[\pm30/0/\text{-}30/0/30/0_4/30/0/\text{-}30/0/\text{-}30/30/d]_S$, where *d* locates the crack plane;
- ❑ Lay-up A[++30]: $[\pm30/0_6/0_6/\text{-}30/30/d]_S$, where *d* locates the crack plane.

The model includes 6800 composite volume elements, 11232 nodes, and 91008 degrees of freedom. A refinement is defined in the vicinity of the crack front: the length and width of the elements is 0.5mm by 0.5mm. Four elements are used over the total beam thickness; the 2 layers of elements touching the crack have each a 0.127 mm thickness. A load of 10 N is applied via a RBE element at the tips of the beam.

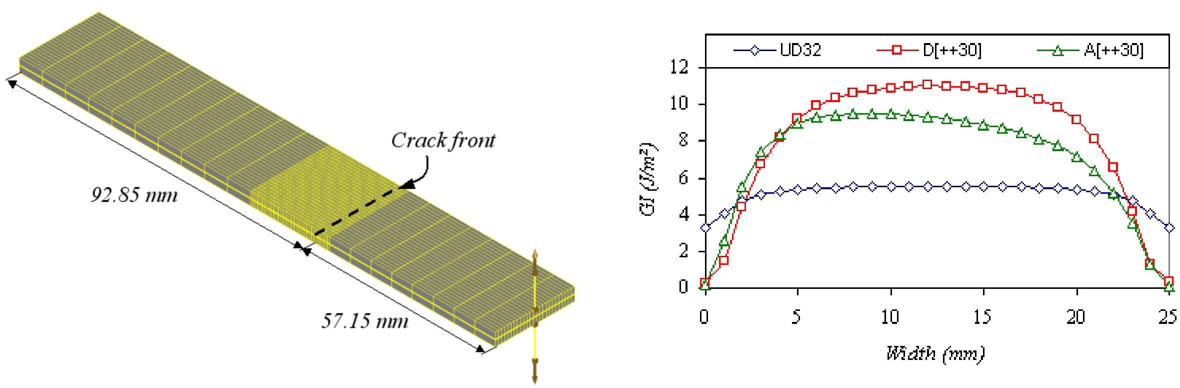

Figure 5. The model of the DCB specimen and the results with the VCE approach

4.3 Mixing shell and volume elements in the model in an ENF test

In order to decrease the size of the problem, volume elements are only used in the vicinity of the crack front while shells are considered elsewhere. This allows saving time while keeping very accurate results. Very small differences in the results may come from the assumptions related to the different finite elements. Here the ENF test is solved with the VCE formulation. The results with a model including only volume elements are compared to the ones obtained when mixing shells and volumes in Figure 6. The specimen width is of 25 mm, while the crack length is 31.75 mm. A ply thickness of 0.127 mm is used, and the material is graphite/epoxy C12K/R6376. The stacking sequence comes from [13]:

- ❑ Lay-up D[+-30]: $[\pm30/0/\text{-}30/0/30/0_4/30/0/\text{-}30/0/\text{-}30/30/d/\text{-}30/30/0/30/0/\text{-}30/0_4/\text{-}30/0/30/0/\pm30]$.

The model with volume elements includes 100059 degrees of freedom. When shells and volumes are used, it goes down to 63318, leading to some computational time savings.

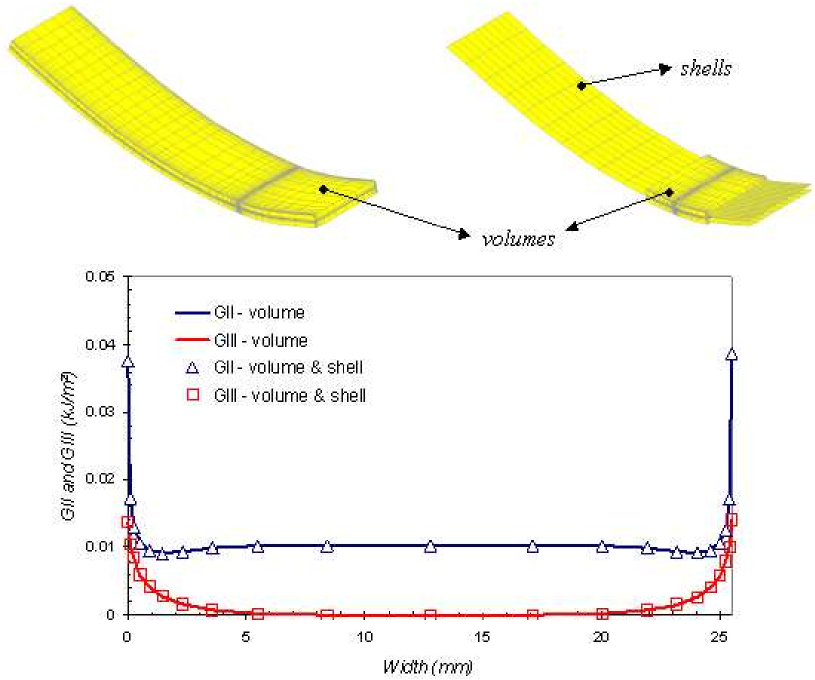

Figure 6. Results for the ENF test with and without shell elements

4.4 A discussion on optimisation with respect to damage tolerance

Designing a composite structure with respect to damage tolerance is becoming a challenge. Although simplified formulations may be used at a global level (e.g. a wing [14]), more sophisticated high fidelity approaches should be selected when local structural components are studied [15,16].

To assess the damage tolerance of composite constructions a given number of cracks are placed in the numerical model and the propagation load is evaluated. This provides an idea to the designer about the resistance of its layered structure in such an unfavourable case. This unfavourable cracked configuration could be the starting point of an optimisation procedure looking for the best stacking sequence of a composite able to support the presence of cracks, by increasing the allowable propagation load and the overall residual stiffness.

Such a formulation is tested on the ENF specimen. The objective to be minimized is the total energy release rate over the crack front. Therefore, minimum, mean and maximum values are minimized, in order to obtain a laminate less prone to see its crack propagate. Only one design variable is selected: it is the angle of the following lay-up:

- Lay-up D[+-θ]: $[\pm\theta /0/-\theta /0/\theta /0_4/\theta /0/-\theta /0/-\theta /\theta /d/-\theta /\theta /0/\theta /0/-\theta /0_4/-\theta /0/\theta /0/\pm\theta]$.

The initial value of θ is 30°, i.e. the initial stacking sequence is a D[+-30].

The inter-laminar toughness depends on the fibres orientations across the interface. Here, in a simplified approach a constant value of G_c is considered. For a sake of accuracy this variation of G_C should of course be included in the formulation of the optimisation problem. The current approach is therefore not rigorous and aims more at comparing optimisation methods. The results should be interpreted with care.

A specific gradient based optimisation approach presented in [17] is used in the BOSS Quattro environment [18], and the sensitivities are up-to-now computed by finite differences. The results of the iterative optimisation process are provided in Figure 7. The optimal value of θ is obtained after 8 iterations, and 15 structural analyses.

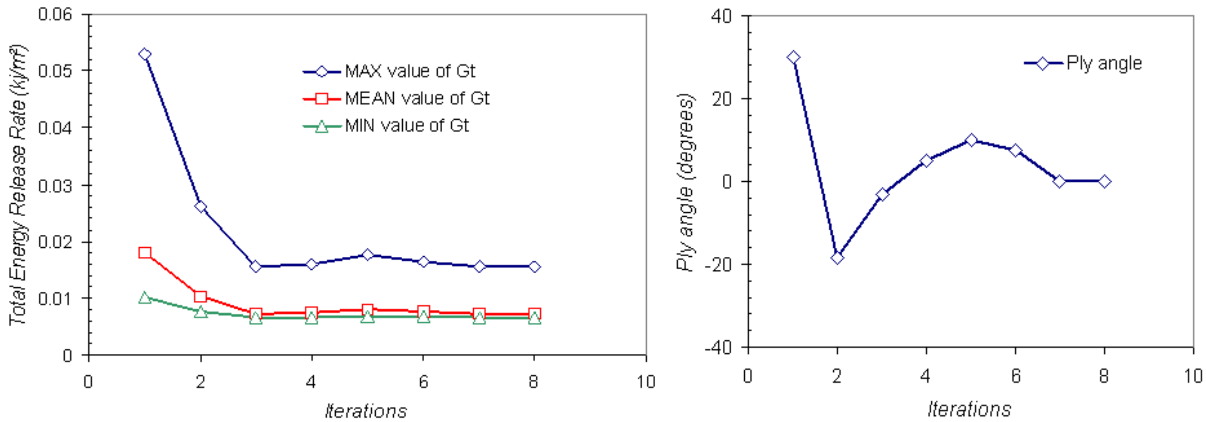

Figure 7. Convergence history with the gradient based method

Surrogate Based Optimisation methods [18] where neural networks are used to generate a global approximation of the design problem, could be efficient for treating the non linear damage problem, as it was the case in [19] for post-buckling optimisation of composite structures. Their advantage is to run analyses in parallel, what is not possible with a sequential gradient based approach. Using such a method provides the same solution within 63 structural analyses, which is competitive with the previous optimisation method since 4 processors were used for the parallel solution (Figure 8).

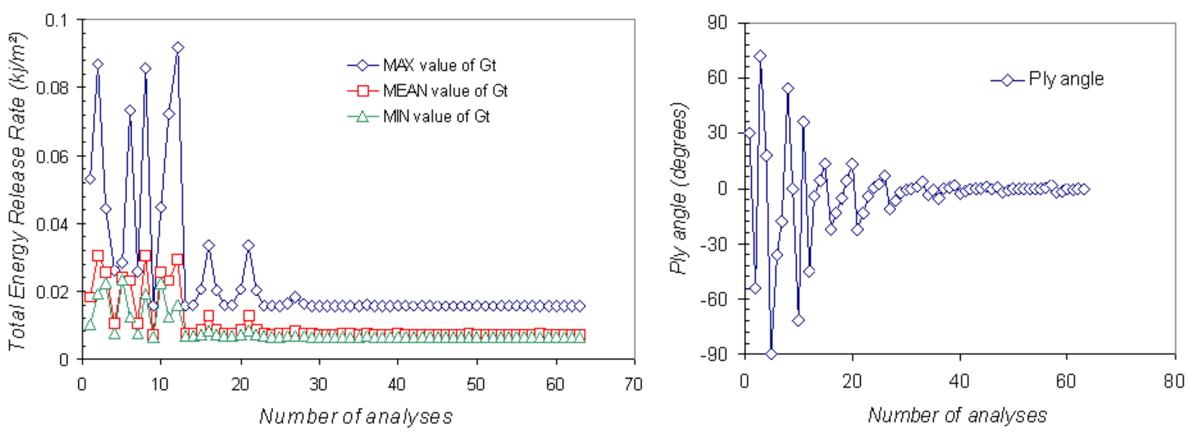

Figure 8. Convergence history with the surrogate based optimisation method

5 Application to a complex (industrial) case

The following example illustrates the cohesive elements approach presented in this paper. In the T-section laminated composite structure depicted in Figure 9, we decided to consider arbitrarily 55 crack fronts located in the skin, the cap and the noodle. The stacking sequences include plies oriented at 0°, +45°, -45° and 90°. The structure is subjected to a pull test. Contact conditions are defined between the delaminated plies. Cohesive elements are here inserted in the model by identifying specific groups of inner faces in the mesh. The nodes are split and interface elements are automatically inserted. The same procedure is used to define the cracks: here however interface elements are removed, leaving double coincident nodes.

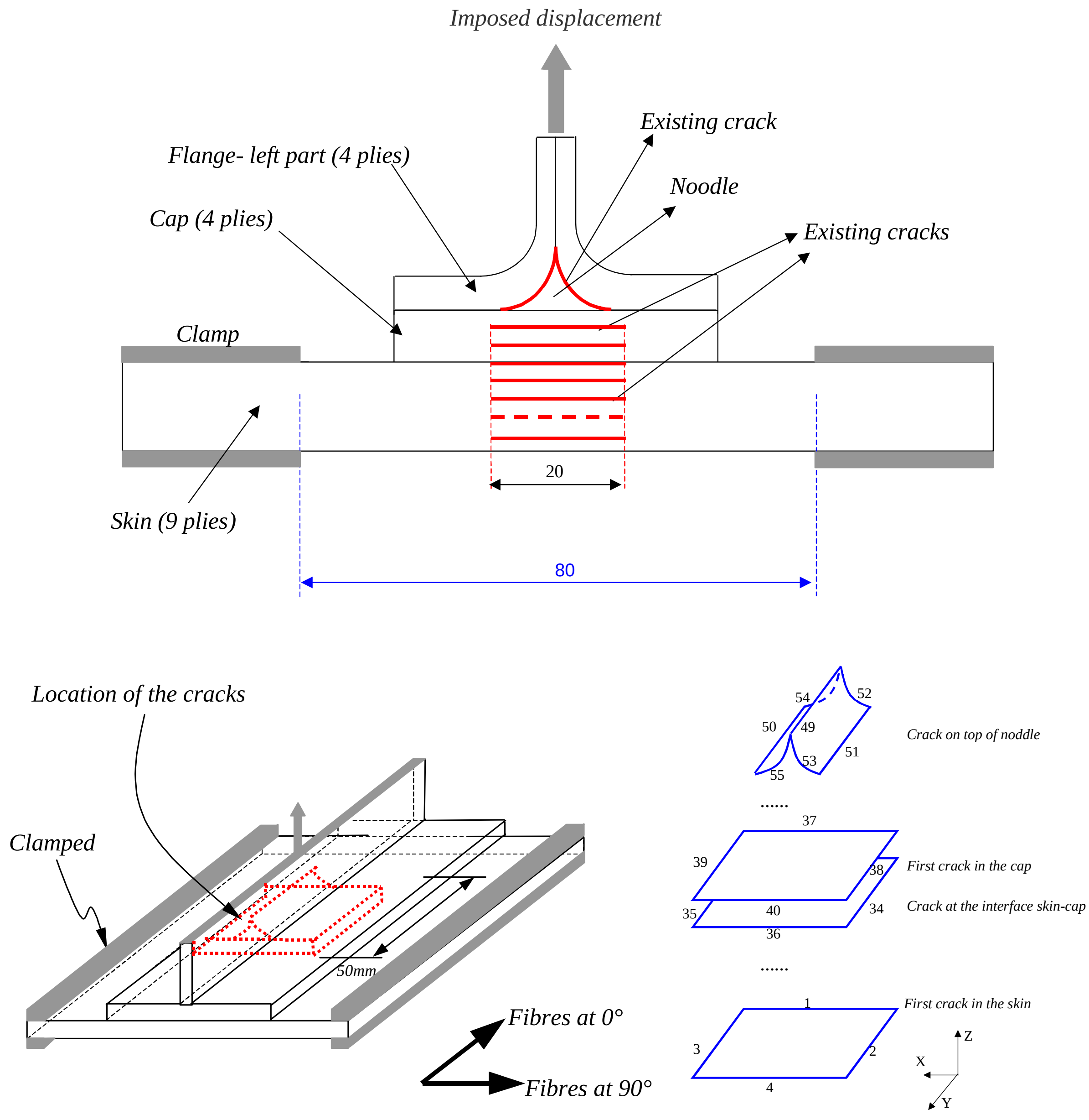

Figure 9. Definition of the problem solved with the cohesive elements approach

The bi-triangular cohesive law of Figure 3 is used. The model includes 293332 degrees of freedom (64574 nodes, 18880 first order volume elements, 12664 2D interface elements and 1221 contact elements). The displacement of the stiffener is imposed via a Rigid Body Element defined on its upper face.

Results are presented in Figures 10 and 11. The maximum carrying load is 9070N. Although a first damage appears between the noodle and the stiffener, the structure fails due to a de-cohesion between the cap and the stiffener. A propagation load of about 4800 N is obtained, corresponding to the first damage reaching 0.99. The initial crack propagation appears for cracks 52 to 55 of Figure 9.

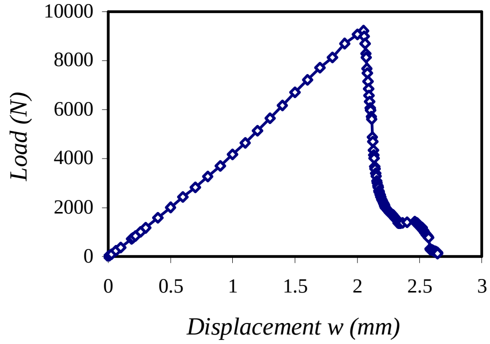

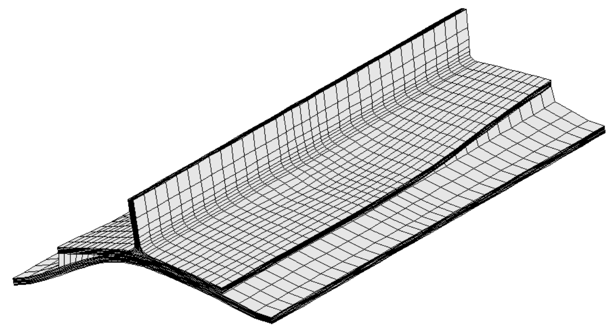

Figure 10. Load-displacement curve and global deformation of the structure
(amplification factor for deformation = 5)

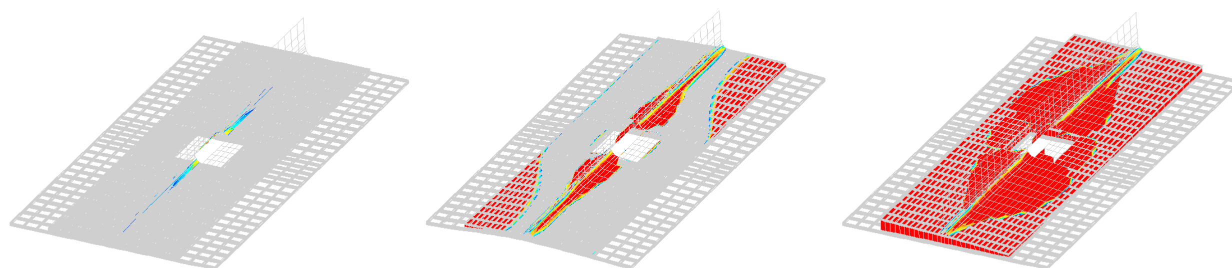

Displacement = 1.5 mm
Load = 6698 N

Displacement =2.1 mm
Load = 6317 N

Displacement = 2.64 mm
Load = 127 N

Figure 11. Evolution of the damage over the loading

6 Conclusions

This paper discussed the methodologies available in SAMCEF for studying and designing complex (industrial) composite structures with respect to delamination. At an industrial level, some needs can be identified, such as large size finite element models, several tens of cracks in the structure, modelling contact conditions over large regions, obtaining accurate results and disposing of efficient optimisation tools.

Through the proposed applications and the related references, it is demonstrated that SAMCEF efficiently answers to those industrial concerns: easy definition of cracks and delamination zones; quick estimation of the propagation load via the VCE method; more advanced capabilities with the cohesive elements approach for inter-laminar cracks propagation and estimation of the overall structural behaviour during the fracture process; library of softening material laws for interlaminar behavior; efficient strategies for treating contact conditions; accurate results (compared to reference solutions); parallel solution procedure for large scale problems.

Additionally, the optimisation facilities of BOSS Quattro helps the engineer in designing its composite structures with respect to, amongst others, damage tolerance criteria.

References

[1] P.P. Camanho. Finite element modelling of fracture in composites: current status and future developments, *NAFEMS Seminar – Prediction and Modelling of Failure Using FEA*, May 31 – June 1, 2006, Roskilde, Denmark.

[2] R. Krueger. Computational fracture mechanics for composites – State of the art and challenges, *NAFEMS Seminar – Prediction and Modelling of Failure Using FEA*, May 31 – June 1, 2006, Copenhagen/Roskilde, Denmark.

[3] R. Krueger. Virtual Crack Closure Technique: history, approach and applications. Applied mechanics Reviews, 57:109-143, 2004.

[4] R. Krueger. An approach for assessing delamination propagation capabilities in commercial finite element codes. *Americam Society of Composites 22nd Annual Technical Conference*, University of Washington, Seattle, WA, September 17-19, 2007.

[5] P. Ladevèze, O. Allix, B. Douchin and D. Lévêque. A computational method for damage intensity prediction in a laminated composite structure, *Computational Mechanics – New Trends and Applications* (Idelsohn S., Oñate E. and Dvorkin E., eds.), CIMNE, Barcelona, Spain, 1998.

[6] V.Q. Bui, E. Maréchal and H. Nguyen Dang. Imperfect interlaminar interfaces in laminated composites : delamination with the R-curve effect. *Composite Science & Technology*, 60:2619-2630, 2000.

[7] A. Pantano and R.C. Averill. Finite element interface technology for modelling delamination growth in composite structures. *AIAA Journal*, 42:1252-1260, 2004.

[8] P. Camanho, C.G. Davila and D.R. Ambur. Numerical simulation of delamination growth in composite materials. NASA-TP-211041, 2001.

[9] SAMCEF. Système d'Analyse des Milieux Continus par Eléments Finis. www.samcef.com

[10] M. Bruyneel, P. Morelle and Delsemme J.P. Failure analysis of metallic and composite structures with SAMCEF. *NAFEMS Seminar – Materials Modelling: FE Simulations of the Behavior of Modern Industrial Materials Including their Failure*, December 5 – 6, 2006, Wiesbaden, Germany.

[11] P. Thévenet. Tolérance aux dommages des structures aéronautiques – Délaminage dans les stratifiés monolithiques et flambage des structures minces. *10th SAMTECH Users Conference*, Palais des Congrès, Liège, March 13-14, 2007.

[12] P. Jetteur. Modèle matériau pour l'élément d'interface. SAMTECH Report RS-246. 2006.

[13] R. Krueger. Three dimensional finite element analysis of multidirectional composites DCB, SLB and ENF specimens. ISD-Report N° 94/2, 1994.

[14] L. Krog, M. Bruyneel, A. Remouchamps and C. Fleury. COMBOX: a distributed computing process for optimum pre-sizing of composite aircraft box structures. *10th SAMTECH Users Conference*, Palais des Congrès, Liège, March 13-14, 2007.

[15] B. Colson, M. Bruyneel, S. Grihon, P. Jetteur, P. Morelle and A. Remouchamps. Composite panel optimization with non linear analysis and semi-analytical sensitivities. *NAFEMS Seminar – Simulating Composite Materials and Structures*, November 6-7, Bad Kissingen, Germany.

[16] M. Bruyneel. Optimization of laminated composite structures: problems, solution procedures and applications. *Composite materials Research Progress*, NOVA Science Publishers, 2008.

[17] M. Bruyneel. A general and effective approach for the optimal design of fibers reinforced composite structures. *Composites Science & Technology*, 66: 1303-1314, 2006.

[18] A. Remouchamps, S. Grihon, C. Raick, B. Colson and M. Bruyneel. Numerical optimisation: a design space odyssey. *International Workshop 2007: Advancements in Design Optimization of Materials, Structures and Mechanical Systems*, Xi'an, China, December 17-20, 2007.

[19] L. Lanzi and V. Giavotto. Post-buckling optimisation of composite stiffened panels: computationsand experiments. *Composite Structures*, 73: 208-230, 2006.